

OPTICAL AND INFRARED NON-DETECTION OF THE $z=10$ GALAXY BEHIND ABELL 1835

GRAHAM P. SMITH,¹ DAVID J. SAND,¹ EIICHI EGAMI,² DANIEL STERN,³ AND PETER R. EISENHARDT³

Draft version February 5, 2008

ABSTRACT

Gravitational lensing by massive galaxy clusters is a powerful tool for the discovery and study of high redshift galaxies, including those at $z \geq 6$ likely responsible for cosmic re-ionization. Pelló et al. recently used this technique to discover a candidate gravitationally magnified galaxy at $z=10$ behind the massive cluster lens Abell 1835 ($z=0.25$). We present new Keck (LRIS) and *Spitzer Space Telescope* (IRAC) observations of the $z=10$ candidate (hereafter #1916) together with a re-analysis of archival optical and near-infrared imaging from the *Hubble Space Telescope* and VLT respectively. Our analysis therefore extends from the atmospheric cut-off at $\lambda_{\text{obs}} \simeq 0.35 \mu\text{m}$ out to $\lambda_{\text{obs}} \simeq 5 \mu\text{m}$ with *Spitzer*/IRAC. The $z=10$ galaxy is not detected in any of these data, including an independent reduction of Pelló et al.'s discovery H - and K -band imaging. We conclude that there is no statistically reliable evidence for the existence of #1916. We also assess the implications of our results for ground-based near-infrared searches for gravitationally magnified galaxies at $z \gtrsim 7$. The broad conclusion is that such experiments remain feasible, assuming that space-based optical and mid-infrared imaging are available to break the degeneracy with low redshift interlopers (e.g. $z \sim 2-3$) when fitting spectral templates to the photometric data.

Subject headings: cosmology:observations — early universe — galaxies: evolution — galaxies: formation — infrared: galaxies

1. INTRODUCTION

Observations of distant QSOs (Becker et al. 2001; Fan et al. 2002) and the cosmic microwave background (Kogut et al. 2003) together suggest that the universe was re-ionized somewhere between $z \simeq 6$ and $z \simeq 20$. Searching for the sources of re-ionizing photons is currently an intense observational effort. Most searches naturally concentrate on luminous systems, i.e. QSOs and luminous galaxies, at $z \sim 6-8$ as these should be easier to detect than less luminous and more distant objects. However QSOs likely produced insufficient photons to accomplish re-ionization alone (Fan et al. 2001; Barger et al. 2003), and the same may be true of luminous ($L \gtrsim 0.3 L^*$ at $z \sim 3.8$) galaxies based on small samples from the *Hubble Space Telescope* Ultra Deep Field (hereafter *HST* UDF; Bouwens et al. 2004; Bunker et al. 2004; Yan et al. 2004). This raises the important possibilities that re-ionization either occurred much earlier, or that the bulk of the re-ionizing photons were emitted by sub-luminous galaxies, i.e. $L \lesssim 0.1 L^*$.

The UDF studies operate close to the detection threshold of the deepest optical/near-infrared imaging available. It is therefore difficult to envisage substantial progress in the detection of more remote and/or less luminous galaxies via deep imaging of “blank fields” with the current generation of telescopes. With the advent of the *James Webb Space Telescope* still some years ahead, the magnifying power of massive galaxy cluster lenses is therefore a much needed boost for the discovery power of *HST* and large ground-based telescopes. Indeed, the galaxy redshift record has been broken on several occasions with the help of the gravitational magnification of distant galaxies by foreground galaxy clusters (Mellier et al. 1991; Franx et al. 1997; Hu et al. 2002; Kneib et al. 2004).

The faint end of the luminosity function of Lyman- α emitters at $z=5$ has also been constrained with the help of gravitational lensing (Santos et al. 2004; Ellis et al. 2001). Extension of these techniques to $z \gtrsim 7$ is therefore an important element of observational studies of cosmic re-ionization.

Pelló et al. (2004 – hereafter P04) reported a gravitationally magnified ($\mu \sim 25-100$) galaxy at $z=10$ (hereafter #1916, following P04's nomenclature) behind the foreground galaxy cluster A 1835 ($z=0.25$). This interpretation is based on non-detection in optical imaging from the ground (3σ limits in a $0.6''$ diameter aperture: $V \geq 27.4$, $R \geq 27.5$, $I \geq 26.9$) and space (3σ limit in a $0.2''$ diameter aperture: $R_{702} \geq 27.2$), and the shape of the continuum at $\lambda_{\text{obs}} \geq 1 \mu\text{m}$ (using a $1.5''$ aperture: $(J-H) \geq 0.6$, $(H-K) = -0.5 \pm 0.4$) which is reminiscent of the Lyman-break selection technique (Steidel et al. 1996). P04 corroborated the putative Lyman-break redshifted to $\lambda_{\text{obs}} \simeq 1.3 \mu\text{m}$ with an emission line at $\lambda_{\text{obs}} = 1.3375 \mu\text{m}$ with integrated flux of $(4.1 \pm 0.5) \times 10^{-18} \text{erg cm}^{-2} \text{s}^{-1}$, which they interpret as Lyman- α . Lower redshift interpretations of the line ([OII] at $z=2.59$; [OIII] at $z=1.68$; $H\alpha$ at $z=1.04$) were discarded by P04 largely on the basis of the low probability of solutions at $z \lesssim 7$ when fitting synthetic spectral energy distributions (SEDs) to their photometric data. The most likely of these lower-redshift solutions ($z=2.59$) was further excluded on the basis of the dust extinction required to fit the photometric data ($A_V \geq 2$), and the absence of doublet structure in the observed emission line.

Based solely on the photometry (optical non-detection, red $(J-H)$ and blue $(H-K)$ colors) the $z=10$ interpretation of #1916 is plausible. However P04's preference for this solution over the lower redshift alternatives was controversial from the outset. For example, the emission line does not have the characteristic P-Cygni profile of Lyman- α , and the different photometric apertures adopted in the optical ($0.6''$ – smaller than the ground-based seeing disc) and near-infrared ($1.5'' - 3 \times$ the seeing disk) may suppress the likelihood of lower-redshift solutions when fitting synthetic SEDs. Bremer

¹ Department of Astronomy, California Institute of Technology, Mail Code 105–24, Pasadena, CA 91125. – Email: gps@astro.caltech.edu

² Steward Observatory, University of Arizona, 933 North Cherry Avenue, Tucson, AZ 85721.

³ Jet Propulsion Laboratory, California Institute of Technology, 4800 Oak Grove Drive, MS 169–327, Pasadena, CA 91109.

et al. have also suggested that #1916 may either not exist, or be intrinsically variable, based on their non-detection in the H -band with NIRI on Gemini-North, $H(3\sigma) > 26$, in contrast to P04's 4σ detection of $H=25.00 \pm 0.25$ with ISAAC on VLT. The spectroscopic identification of #1916 is also in doubt. Weatherley et al. (2004) re-analyzed P04's spectroscopic data and failed to detect the emission line at $\lambda_{\text{obs}} = 1.3375 \mu\text{m}$, citing spurious positive flux arising from variable hot pixels in the ISAAC array as the likely source of the discrepancy.

A 1835 has been used previously as a gravitational telescope, for example targeting sub-millimeter galaxies (hereafter SMGs; e.g. Smail et al. 2002) and galaxies with extremely red optical/near-infrared colors (Smith et al. 2002). One of the galaxies detected in these surveys, SMMJ 14011+0252, lies at $z=2.56$ and suffers an estimated extinction of $1.8 \lesssim A_V \lesssim 6.5$ (Ivison et al. 2000). Bearing in mind recent discovery of galaxy groups at $z \sim 2-3$ associated with gravitationally lensed SMGs (Kneib et al. 2004; Borys et al. 2004), and the strong clustering of SMGs (Blain et al. 2004), #1916 is plausibly at a similar redshift to SMMJ 14011+0252, and may also be obscured by dust. Further circumstantial evidence for a lower redshift interpretation of #1916 comes from Richard et al. (2003) who used the same spectroscopic data as presented by P04 to discover a strongly reddened star-forming galaxy at $z=1.68$. This redshift coincides with the [OIII] interpretation of P04's putative emission line at $\lambda_{\text{obs}} = 1.3375 \mu\text{m}$.

In this paper, we address three questions: (i) is #1916 at $z \sim 2-3$?; (ii) is #1916 intrinsically variable?; (iii) does #1916 exist? These tests exploit new optical and mid-infrared observations using the Keck-I 10-m telescope and the *Spitzer Space Telescope* respectively, plus an independent reduction of P04's H - and K -band imaging data from VLT. Throughout this article we assume that the emission line at $\lambda_{\text{obs}} = 1.3375 \mu\text{m}$ is a false detection (Weatherley et al. 2004). In §2 we present the new Keck and *Spitzer* data, explain in detail the re-reduction of the archival VLT/ISAAC data, and summarize the archival *Hubble Space Telescope* (*HST*) data. Then in §3 we describe the analysis and key results, focusing on the three questions posed above; this section closes with a summary of the current observational status of #1916. Finally, we discuss the implications of our results for future ground-based near-infrared searches for galaxies at $z \gtrsim 7$ (§4) and summarize our conclusions in (§5).

We assume $H_0 = 65 \text{ km s}^{-1} \text{ Mpc}^{-1}$, $\Omega_M = 0.3$ and $\Omega_\Lambda = 0.7$ throughout. Unless otherwise stated all error bars are at 1σ significance; photometric detection limits are at 3σ significance; upper and lower limits on colors are based on 3σ detection thresholds in the non-detection filter. Magnitudes are stated in the AB system; conversion between the AB and Vega systems for the specific filters used in this paper are as follows:- $\Delta_B = B_{\text{AB}} - B_{\text{Vega}} = -0.1$, $\Delta_V = 0.1$, $\Delta_R = 0.2$, $\Delta_{F702W} = 0.3$, $\Delta_I = 0.5$, $\Delta_J = 0.9$, $\Delta_H = 1.4$, $\Delta_K = 1.9$, $\Delta_{3.6\mu\text{m}} = 2.8$, $\Delta_{4.5\mu\text{m}} = 3.2$.

2. OBSERVATIONS AND DATA REDUCTION

We describe new and archival observations of #1916 in order of increasing wavelength, spanning the observed optical, near-infrared and mid-infrared: spectroscopy with LRIS on Keck-I ($0.35 \leq \lambda_{\text{obs}} \leq 0.95 \mu\text{m}$); imaging with WFPC2 on-board *HST* ($\lambda_{\text{obs}} = 0.7 \mu\text{m}$); near-infrared imaging with ISAAC on ESO's VLT ($\lambda_{\text{obs}} = 1.6 \mu\text{m}$ and $2.2 \mu\text{m}$); IRAC/*Spitzer* observations at $\lambda_{\text{obs}} = 3.6 \mu\text{m}$ and $4.5 \mu\text{m}$.

The detection of any optical flux from #1916 would elim-

TABLE 1
SUMMARY OF PHOTOMETRY

Filter	Telescope/ Instrument	FWHM ($''$)	Aperture Photometry ^a	
			Pelló et al. ^b	This Paper
V	CFHT/12k	0.76	$\geq 27.5 (0.6'')$...
R	CFHT/12k	0.69	$\geq 27.6 (0.6'')$...
R_{702}	<i>HST</i> /WFPC2	0.17	$\geq 27.2 (0.2'')$ ^c	$\geq 27.0 (0.5'')$
I	CFHT/12k	0.78	$\geq 26.0 (0.6'')$...
J	VLT/ISAAC	0.65	$\geq 25.6 (1.5'')$...
H	VLT/ISAAC	0.50	$25.00 \pm 0.25 (1.5'')$	$\geq 25.0 (1.5'')$
K	VLT/ISAAC	0.38	$25.51 \pm 0.36 (1.5'')$	$\geq 25.0 (1.5'')$
$3.6 \mu\text{m}$	<i>Spitzer</i> /IRAC	1.7	...	$\geq 24.3 (5.1'')$
$4.5 \mu\text{m}$	<i>Spitzer</i> /IRAC	1.7	...	$\geq 24.3 (5.1'')$

^a Each number in parentheses is the diameter of the aperture used for the respective photometric measurements. In §4 P04's optical non-detections are re-scaled to a photometric aperture of $2''$ diameter (~ 3 times the seeing disc): $V \geq 26.2$, $R \geq 26.3$, $I \geq 24.7$.

^b We convert all of P04's optical detection limits and their 1σ J -band detection to 3σ limits.

^c P04 do not state whether their R_{702} detection limit is in the Vega or AB system. We have assumed the former and converted it to AB in this table. P04 also do not explain how they reduced the WFPC2 data, specifically whether the final pixel scale was different from the native $0.0996''/\text{pix}$ of the WFC detectors. In this table we have assumed that the four pixels over which this detection limit is measured (see P04 §2.1) subtend a solid angle of $0.0996'' \times 0.0996''$. Given these uncertainties and the absence of this detection limit from P04's Table 1 and Fig. 3, we ignore P04's limit when attempting to reproduce their photometric redshift results in §4.

inate the $z=10$ interpretation (e.g. Stern et al. 2000). In contrast, optical non-detection would have several alternative interpretations, including: a galaxy at $z=10$ as per P04; a dusty galaxy at $z \sim 2-3$; non-existence of #1916. The mid-infrared observations (§2.4) should therefore help to constrain the amount of energy re-radiated by dust in the $z \sim 2-3$ interpretation, and our re-reduction of P04's VLT data also helps to clarify the possibility that #1916 may not exist, or may be variable (Bremer et al. 2004). The Keck and *Spitzer* data described in this section were collected and analyzed in parallel with those presented by Bremer et al. (2004).

2.1. Keck Spectroscopy

As part of a broad effort to secure spectroscopic redshifts of gravitational arcs spanning several observational programs (Smith et al. 2001, 2002, 2005; Sand et al. 2002, 2004, 2005; Edge et al. 2003; Sharon et al. 2005), we observed A 1835 with the Low Resolution Imager Spectrograph (LRIS; Oke et al. 1995) in multi-slit mode on the Keck-I 10-m telescope⁴ on UT 2004 March 29. A single mask was observed, including a slit targeting #1916. The purpose of this slit was to search for line emission in the $0.35 \leq \lambda_{\text{obs}} \leq 0.95 \mu\text{m}$ wavelength range. For example, if #1916 does indeed lie at $z \sim 2.6$ (§1), then Lyman- α may be detectable at $\lambda_{\text{obs}} \simeq 0.44 \mu\text{m}$.

The observations totaled 3.6-ks, split into two exposures, using the D560 dichroic with the 400/8500 grating and the 400/3400 grism. On the red side the spectral dispersion was $1.86 \text{ \AA}/\text{pixel}$ with a pixel scale of $0.214''/\text{pixel}$ and on the blue side the spectral dispersion was $1.09 \text{ \AA}/\text{pixel}$ with a pixel scale of $0.135''/\text{pixel}$. Overhead conditions were moderate ($\text{FWHM} \simeq 1''$), and probably not photometric, however a flux

⁴ The W. M. Keck Observatory is operated as a scientific partnership among the California Institute of Technology, the University of California, and NASA.

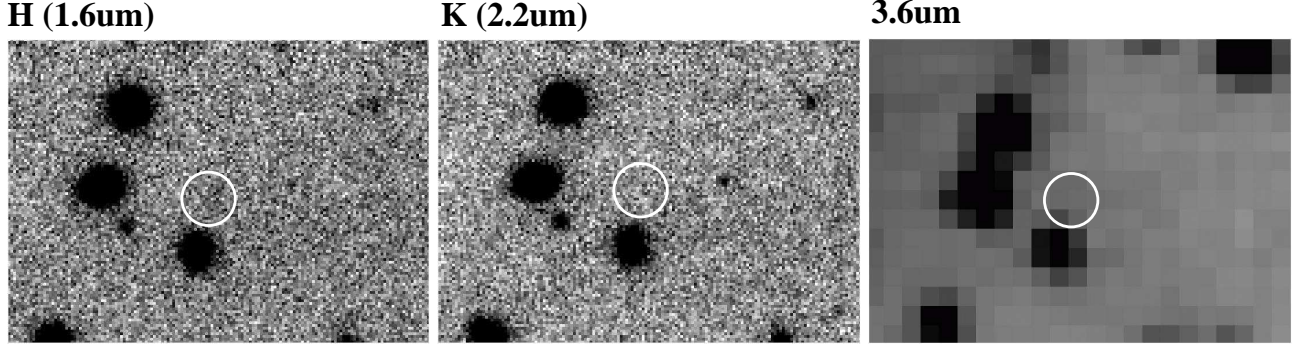


FIG. 1.— Infrared images of the $z=10$ candidate at 1.6, 2.2, and $3.6\mu\text{m}$ respectively. The two left panels are based on our independent re-reduction of P04’s ISAAC data described in §2.3. The white circles mark the position of #1916 from P04 – there is no obvious sign of flux in any of these panels. Formal 3σ detection limits are: $H \geq 25$, $K \geq 25$, $F \leq 0.75\mu\text{Jy}$. North is up and East left. Each panel is $23'' \times 16''$.

calibration was obtained using the spectrophotometric standard star HZ44 (Oke et al. 1990). The data were de-biased, flat-fielded, sky-subtracted, extracted and calibrated in a standard manner within IRAF⁵.

No flux at observed optical wavelengths has yet been detected at the position of #1916 (P04; Lehnert et al. 2004; §2.2). We therefore did not expect to detect any continuum emission, and concentrated instead on searching for faint emission lines of large equivalent width. Visual inspection of the reduced 2D data revealed neither continuum nor line emission. To estimate the sensitivity limit we extracted a 1D trace from the center of the slit corresponding to the full width of the seeing disk, and estimated the 3σ detection limit per 5-Å spectral resolution element to be $\sim 4.5 \times 10^{-19} \text{ erg s}^{-1} \text{ cm}^{-2}$ at $\lambda_{\text{obs}} = 0.44\mu\text{m}$ – i.e. the observed wavelength at which Lyman- α would be found if #1916 is at $z=2.6$.

2.2. Archival Hubble Space Telescope Imaging

A 1835 has also been observed through the F702W filter with the WFPC2 camera on-board *HST*⁶. We refer the reader to Smith et al. (2005) for details of these data and their reduction. P04 do not detect #1916 in these data (Table 1), although they neither explain how they reduced the data nor how the detection limit was calculated. Here, we use Smith et al.’s (2005) reduced frame which has a pixel-scale of $0.0498''/\text{pixel}$ after drizzling. To simplify the analysis, we re-bin the data back to the original pixel-scale of $0.0996''/\text{pixel}$ to minimize the impact of pixel-to-pixel correlations in the background noise when estimating the sensitivity limit of the data.

Visual inspection reveals no obvious flux at the position of #1916 in these data. To quantify this non-detection, we follow the same procedure as P04 – we measured the background noise in apertures placed randomly into blank sky regions of both frames near to the position of #1916. We ensure consistency with other wavelengths by matching the diameter of these apertures to a diameter $3\times$ that of the seeing disk, i.e. $0.5''$. We obtain a 3σ sensitivity limit in that aperture of $R_{702}=27.0$ (Table 1).

2.3. Archival VLT/ISAAC Imaging

⁵ IRAF is distributed by the National Optical Observatories, which is operated by the Association of Universities for Research in Astronomy, Inc. (AURA) under cooperative agreement with the National Science Foundation.

⁶ Based in part on observations with the NASA/ESA *Hubble Space Telescope* obtained at the Space Telescope Science Institute, which is operated by the Association of Universities for Research in Astronomy, Inc., under NASA contract NAS 5-26555.

Deep near-infrared imaging of A 1835 was obtained by P04 with the ISAAC 1024×1024 Hawaii Rockwell array on ESO’s 8-m VLT⁷ in February 2003. We reduced independently the H - and K -band data using standard IRAF tasks, paying careful attention to rejection of cosmetic defects in the ISAAC array, including bad pixels, and to conserving the noise properties of the data. We detail key features of the data reduction below.

- (i) Flat-fielding and sky-subtraction were combined into a single step using a median of the eight frames temporally adjacent to each science frame. We refer to this step as “flat-fielding”, and to the rolling temporal median frames as “sky-flats”.
- (ii) Flat-fielding was performed twice. First on the dark-subtracted frames which were then registered and averaged to produce a first-pass reduced frame. This frame was then used to mask out flux from identified sources from the individual dark-subtracted frames, and these masked frames were then used to construct the sky-flats in a second-pass reduction. This approach minimizes the loss of flux from objects with angular extents comparable with the size of the dither pattern. This is important when searching for faint objects along lines-of-sight through the crowded cores of rich galaxy clusters because the light from bright cluster galaxies effectively form a spatially varying background against which the faint sources are detected. The goal of the second-pass flat-field is to conserve this “background”.
- (iii) Independent bad pixel masks were made by sigma-clipping both the darks and the sky-flats. The former identifies 22,020 pixels (2.1% of the total array) as static, i.e. “bad”, and the latter identifies the same 22,020 pixels plus an additional 12,373 pixels (a further 1.2% of the total array) as bad. The latter mask was adopted as the fiducial bad pixel mask.
- (iv) Detector bias residuals were removed by subtracting the median along rows in individual flat-fielded frames after masking identified sources, in a manner similar to that described by Labbé et al. (2003).
- (v) The individual frames were integer pixel aligned. This has the important benefit of minimizing pixel-to-pixel

⁷ Based in part on observations collected with the ESO VLT-UT1 Antu Telescope.

correlations in the noise properties of each frame and thus the final stacked frame. Calculation of the background noise is therefore simplified relative to a reduction scheme based on sub-integer pixel alignment of the individual frames.

- (vi) No frames were rejected when making the final combination of the reduced, aligned frames. Two versions of the final stacked frame were made: a straight average and a weighted average – the weight of an individual frame was proportional to $(\sigma \times \text{rms})^{-2}$, where σ is the FWHM of the seeing disk, and rms is the root mean square per pixel of the noise in each frame. The weighted version of the final frame has slightly better image quality than the straight average. We therefore adopt it for the analysis described below.

The final reduced H - and K -band frames have seeing of $\text{FWHM}=(0.45 \pm 0.01)''$ and $\text{FWHM}=(0.34 \pm 0.02)''$ respectively. Photometric calibration was achieved with the standard star observations that were interspersed with the science observations as part of P04's original program. We show extracts from the reduced H - or K -band frames in Fig. 1. Visual inspection of both the fits frames and Fig. 1 reveals no obvious flux at the location of #1916 in either the H - or K -band. Following P04 we again randomly insert $1.5''$ diameter apertures (roughly 3 times the seeing disc) into blank sky regions near to the position of #1916, obtaining 3σ sensitivity limits in this aperture of: $H=25.0$ and $K=25.0$.

2.4. Spitzer/IRAC Imaging

A1835 was observed with the InfraRed Array Camera (IRAC; Fazio et al. 2004) on-board *Spitzer*⁸ on UT 2004 January 16 in the 3.6, 4.5, 5.8 and $8.0\mu\text{m}$ channels. Here we discuss the two shortest wavelength, more sensitive, observations. Twelve and eighteen 200-second exposures were accumulated at $3.6\mu\text{m}$ and $4.5\mu\text{m}$ respectively, using the small-step cycling dither pattern. The Basic Calibrated Data (BCD) were combined using custom routines to produce the final stacked frame with a pixel scale of $0.6''/\text{pixel}$. We re-binned the data back to the original pixel scale of $1.2''/\text{pixel}$ to eliminate correlations in the background noise.

Visual inspection of the final frames again indicates that there is no flux at the position of #1916 (Fig. 1). To quantify this non-detection we follow the same procedure as P04, as described in §2.2. We used $5.1''$ diameter apertures, i.e. $3 \times$ the seeing disk of the IRAC observations to obtain 3σ sensitivity limits of: $F(3.6\mu\text{m})=0.75\mu\text{Jy}$ and $F(4.5\mu\text{m})=0.75\mu\text{Jy}$ respectively.

3. ANALYSIS AND RESULTS

The objective of this section is to answer the three questions posed in §1: (i) is #1916 at $z \sim 2-3$?; (ii) is #1916 intrinsically variable?; (iii) does #1916 exist? Preliminary inspection of the data in §2 indicates that no flux is detected at the position of #1916 at any wavelength to date. Combining this with Bremer et al.'s more sensitive non-detection of $H(3\sigma) > 26.0$, it is tempting to leap to the third question and reply “no”. We adopt a more conservative approach.

⁸ This work is based in part on observations made with the Spitzer Space Telescope, which is operated by the Jet Propulsion Laboratory, California Institute of Technology under a contract with NASA.

3.1. Is #1916 at $z \sim 2-3$?

This test concentrates on the optical data because the detection of any flux shortward of the putative Lyman limit of a galaxy at $z \sim 10$ would immediately discount that interpretation. The red observed optical/near-infrared spectral energy distribution described by P04 could then be naturally explained by a dusty galaxy at $z \sim 2-3$, perhaps associated with the SMGs that lie within $\sim 30''$ ($\sim 200-300\text{kpc}$ in projection at $z \sim 2-3$) of #1916 (Ivison et al. 2000; Smail et al. 2005).

Our new non-detection of #1916 with LRIS (§2.1), coupled with confirmation of P04's non-detection with *HST*/WFPC2 and Lehnert et al.'s non-detection in the V -band with VLT/FORS are mutually consistent in the sense that no optical flux has been detected at this position to date. However these non-detections are consistent with all of the following: $z=10$, extreme dust obscuration at $z \sim 2-3$, an intrinsically variable source, and non-existence. The result of this test is therefore inconclusive.

3.2. Is #1916 Intrinsically Variable?

The objective of this section is to test Bremer et al.'s (2004) proposal that #1916 is intrinsically variable. If P04's photometry ($H=25.00 \pm 0.25$ and $K=25.51 \pm 0.51$) is reproducible using our independent reduction of their near-infrared data, then the variable hypothesis would be supported. If not, then the idea that #1916 does not exist would gain credibility (§3.3).

We attempt to reproduce P04's analysis using SExtractor (Bertin & Arnouts 1996). SExtractor was configured to locate all sources with at least 7 pixels that are $\geq 0.75\sigma$ per pixel above the background – i.e. a signal-to-noise ratio of $\gtrsim 2$ per resolution element, based on the H -band seeing disk of $\text{FWHM}=0.45 \pm 0.01''$ (§2.3) and the $0.15''/\text{pix}$ scale of the ISAAC pixels. We also smoothed the data with a gaussian filter that matched the FWHM of the observed point sources, i.e. a gaussian of $\text{FWHM}=3$ pixels. In this configuration SExtractor failed to detect a source at the position of #1916. We therefore experimented with different smoothing schemes, both increasing and decreasing the full width of the gaussian filter. A “detection” was only possible with the smallest available filter – $\text{FWHM}=1.5$ pixels, i.e. half the width of the seeing disk – yielding $H=25.3 \pm 0.6$. Experimentation with block filters produced similar results in that a “detection” was not possible with any of the standard SExtractor block filters: 3×3 , 5×5 , 7×7 pixels. We also analyzed the K -band data in exactly the same manner and failed to detect anything at the position of #1916 with any gaussian or block filter.

The H -band segmentation map produced when smoothing with the $\text{FWHM}=1.5$ pixel gaussian reveals that the “detection” is very elongated, with a width of 1–2 pixels and a length of ~ 5 pixels. The orientation of these pixels is consistent with the orientation of #1916 reported by P04. It is important to stress that the motivation for filtering data with a kernel that matches the resolution element of the data is to suppress false detections. The collection of pixels identified by SExtractor at the position of #1916 was only “detectable” with a smoothing kernel that has a linear scale half that of the resolution element of the data. It is therefore instructive to consider how many such $\sim 2\sigma$ blobs exist within the ISAAC data. In a single $1.5''$ diameter aperture (i.e. matching that used for the photometry described above) placed randomly in these H -band data, there is a 5% chance of detecting a 2σ noise fluctuation – i.e. a spurious detection. However the ISAAC array (1024×1024 pixels, each pixel $0.15'' \times 0.15''$) contains of or-

der 10^4 independent photometric apertures of $1.5''$ diameter. The H -band frame therefore contains ~ 500 noise fluctuations of 2σ significance.

Sadly, the only reasonable conclusion to draw from this analysis is that #1916 is not detected in our independent reduction of P04's data. We therefore place 3σ limits on the flux at this position of: $H \geq 25.0$ and $K \geq 25.0$ (§2.3). The only wavelength at which two directly comparable observations are available is in the H -band. Combining our non-detection with that of Bremer et al. (2004), we conclude that there is no evidence for variability of #1916, and that (if it exists) its H -band flux is fainter than $H=26$ at 3σ significance (Bremer et al. 2004).

3.3. Does #1916 exist?

The results of the preceding two sections were derived from non-detection of #1916 across the broadest wavelength range to date: $0.35 \leq \lambda_{\text{obs}} \leq 5\mu\text{m}$. We now combine all of these non-detections to address the question of whether #1916 exists. The data force us to conclude that there is no statistically sound evidence that #1916 exists. The balance of probability is that #1916 was a false detection in P04's discovery observations. New observational data yielding statistically sound detections are required before P04's claim that #1916 is the most distant galaxy yet discovered may be resurrected. We consider this unlikely, but we hope to be surprised by Pelló et al.'s forthcoming *HST* observations.

4. DISCUSSION

4.1. The Near-infrared Non-detection

We first discuss possible reasons for the difference between our non-detection of #1916 and P04's ~ 3 – 4σ near-infrared detections. We single out two data reduction steps (§2.3) for discussion – the efficiency of bad pixel rejection and the conservation of noise properties.

4.1.1. Efficiency of bad pixel rejection

The efficiency with which bad pixels are identified can affect estimates of the signal coming from faint sources – if some bad pixels are not identified, they could enhance the flux detected by SExtractor. In §2.3 we used two different methods to identify bad pixels, finding a small but potentially important difference between the two methods. To assess the impact of reduced efficiency of bad pixel identification we made a mask image that contained the 12,373 bad pixels identified only in the bad pixel mask generated from the sky-flats. We then made one copy of the mask per science frame and integer-pixel shifted them to match the observed dither pattern. Finally we took the weighted average of these aligned mask frames and summed the pixel counts in a $1.5''$ diameter aperture centered on #1916. From this we concluded that 7 bad pixels that are only identified in our “sky-flat” bad pixel maps fall within the final photometric aperture. We estimate that if not identified and excluded from the analysis, these pixels could increase the flux estimates by several tenths of a magnitude.

4.1.2. Conservation of noise properties

The approach to re-sampling (or not) the individual frames during the data reduction process, especially the alignment of individual frames affects the noise properties of the final stacked frame. If the individual frames are re-sampled, for example by sub-integer pixel aligning them immediately

prior to producing the final stacked frame, then the noise in the stacked frame is correlated. Such pixel-to-pixel correlations are generally absent from integer-pixel aligned data, thus simplifying the noise properties of the final frame. Neither sub-integer nor integer pixel alignment is intrinsically correct. The relevant issue is correct measurement of the noise in each case – this is critical to assess accurately the statistical significance of sources detected close to the sensitivity limit of the data. Specifically, if the pixel-to-pixel correlations in sub-integer pixel aligned data are not included in the error analysis, then the noise is under-estimated and the statistical significance of the detection over-estimated (Casertano et al. 2000). We integer pixel aligned the individual frames in §2.3 in order to simplify the error analysis. We now estimate by how much we would have under-estimated the noise if we had sub-integer pixel aligned the individual frames and then ignored the pixel-to-pixel correlations when calculating noise level. This is achieved by simply sub-integer aligning the individual frames and re-combining them using a weighted average. Ignoring any resulting pixel-to-pixel correlations, we obtain a 3σ threshold of $H=25.2$, which is slightly fainter than our threshold of $H=25.0$.

In summary, it is plausible that the difference between our near-infrared non-detection and P04's detection of #1916 using the same raw data can at least in part be explained by the efficiency of bad pixel identification and treatment of correlated noise.

4.2. Implications for Future Work

We now discuss the implications of our results for future work, focusing on the feasibility of searches for gravitationally magnified stellar systems at $z \gtrsim 7$ using ground-based near-infrared data. We begin by noting that, had their photometry been reliable, P04's original $z=10$ interpretation of #1916 was plausible, based solely on the photometric data. We therefore adopt P04's optical and near-infrared photometry as being representative of what may be expected from similar future experiments – i.e. optical non-detections in several filters based on a few hours of observations with a 4-m class telescope, a non-detection in a single red optical filter with *HST*, ~ 3 – 4σ detections in two near-infrared filters, and possibly observations with *Spitzer*/IRAC. Specifically, we investigate the degeneracy between $z \gtrsim 7$ interpretations of such datasets with lower redshift alternatives, and how such degeneracies might be broken.

We use Version 1.1 of HYPER-Z⁹ (Bolzonella et al. 2000) to fit standard Bruzual & Charlot (1993) single stellar population models (Burst, E, Sa, Sc, Im) to the photometric data. We assume a Calzetti et al. (2000) extinction law, allow dust extinction in #1916 to lie in the range $0 \leq A_V \leq 4$, adopt $E(B-V) = 0.03$ for extinction within the Milky Way (Schlegel et al. 1998), and use Madau's (1995) prescription for absorption by the inter-galactic medium. In each case described below, if we fit the models to all available photometric information across the full redshift range ($0 \leq z \leq 11$), then we obtain $\chi^2 \lesssim 1$ (all χ^2 values are quoted per degree of freedom) for all redshifts beyond $z \simeq 7$. This is because the models are defined to have zero flux short-ward of the Lyman limit ($\lambda_{\text{rest}} = 0.0912\mu\text{m}$). At $z \gtrsim 6$, the models also have negligible flux short-ward of Lyman- α ($\lambda_{\text{rest}} = 0.1215\mu\text{m}$) due to the Lyman forests and Gunn Peterson absorption. These two

⁹ Available from <http://webast.ast.obs-mip.fr/hyperz>

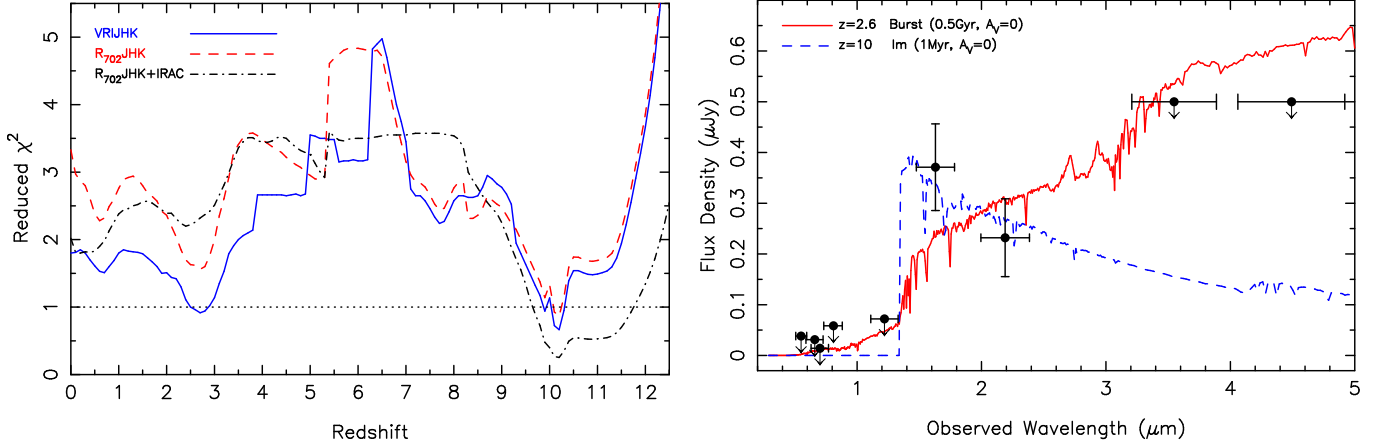


FIG. 2.— LEFT: Reduced χ^2 as a function of photometric redshift and the filters used in the model fits. The red dashed curve has been offset +0.2 in the Y -direction for clarity. This panel demonstrates that P04’s discovery photometry ($VRIJHK$) is degenerate between $z \simeq 2.6$ and $z \simeq 10$ (blue solid curve). Adding in sensitive space-based detection thresholds from *HST* and *Spitzer*/IRAC (red dashed and black dot-dashed curves respectively) lifts this degeneracy. RIGHT: The best-fit spectral templates to the $R_{702}JHK$ -band photometry at $z=2.6$ (red solid) and $z=10$ (blue dashed). The IRAC detection thresholds are also marked to illustrate the power of these data to discriminate between low- and high-redshift interpretations of the shorter wavelength data.

spectral features are progressively redshifted long-ward of the observed optical filters at high redshift, rendering the shorter wavelength detection limits irrelevant to the fits. The goodness of fit is therefore systematically over-estimated at high redshift if all photometric information is included in the fit across the full redshift range. We therefore fit the models to the data in a series of redshift chunks – only the photometric information that lies longward of red-shifted Lyman- α is considered in each redshift chunk. The results described below are insensitive to whether the Lyman limit is substituted for Lyman- α .

First, we fit the models to P04’s $VRIJHK$ -band ground-based photometry (i.e. the $VRIJ$ -band detection limits and the HK -band detections listed in column 4 of Table 1). Note that P04 used different sized apertures for the near-infrared ($1.5''$) and optical ($0.6''$) photometry respectively. We find two acceptable solutions: $z \simeq 2.6$ and $z \simeq 10$ (Fig. 2), neither of which require any dust-obscuration within #1916, the latter having the lower formal χ^2 value. We also scale P04’s ground-based optical non-detections to that appropriate for a consistent photometric aperture of three times the seeing disk at all wavelengths ($V \geq 26.2$, $R \geq 26.3$, $I \geq 24.7$). This marginally improves the goodness of fit of the $z \simeq 2.6$ solution, and is otherwise indistinguishable from the original fit. We retain the matched photometric apertures for the remainder of this analysis.

To improve the discrimination between low- and high-redshift solutions, we add the sensitive *HST*/WFPC2 detection threshold of $R_{702} \geq 27.0$ (Table 1) to the photometric constraints. We fit the synthetic SEDs to the combined $VRR_{702}IJHK$ dataset. The goodness of fit of the $z \simeq 2.59$ solution is marginally worse relative to the $VRIJHK$ -band analysis, because the most stringent optical non-detection comes from the R_{702} -band. However, in general, the χ^2 as a function of redshift is indistinguishable between this fit and the $VRIJHK$ -band fits. This is probably because the χ^2 is dominated by the non-detections in six out of the eight observed filters. To test this we re-fit the models, limiting the data to just the $R_{702}JHK$ -bands, i.e. the most sensitive non-detection (R_{702}), the reddest non-detection (J) and the two detections (HK). The impact of the sensitive detection limit from the

HST data is now clearly evident in the new χ^2 distribution, as shown in Fig. 2. The only acceptable fit to the $R_{702}JHK$ -band data is at $z \simeq 10$.

We show the best fit SEDs at $z=2.6$ and $z=10$, based on the $R_{702}JHK$ -band data in the right panel of Fig. 2. This demonstrates the potential power of IRAC photometry to further discriminate between low and high-redshift interpretations of candidate high-redshift galaxies. The SED of low redshift solutions (e.g. $z \simeq 2.6$) is red at $\lambda_{\text{obs}} \sim 3\text{--}5\mu\text{m}$, and the SED of high redshift solutions ($z \simeq 10$) is blue at similar wavelengths. We add the detection limits obtained at $\lambda_{\text{obs}} = 3.6\mu\text{m}$ and $4.5\mu\text{m}$ to the $R_{702}JHK$ -band data and re-fit the spectral templates. The result is shown in the left panel of Fig. 2 – the reduced χ^2 of the $z \simeq 2.6$ solution is now in excess of 2, and the only redshifts which achieve an acceptable fit to the data are $9.5 \lesssim z \lesssim 11.5$.

In summary, a single sensitive non-detection derived from *HST* imaging, combined with deep ground-based near-infrared imaging and $\sim 2,400$ second integrations with *Spitzer*/IRAC at 3.6 and $4.5\mu\text{m}$ can break the degeneracy between low and high-redshift interpretations of candidate $z \gtrsim 7$ stellar systems (see also Egami et al. 2004; Eyles et al. 2005). Whilst this is not an exhaustive study, it demonstrates that despite the demise of #1916, searches for gravitationally magnified galaxies at extremely high redshifts using ground-based near-infrared data remain feasible when combined with sensitive space-based and mid-infrared data.

5. CONCLUSIONS

We have analyzed new and archival observations of the $z=10$ galaxy #1916 behind the foreground galaxy cluster lens A 1835 ($z=0.25$) spanning $0.35 \leq \lambda_{\text{obs}} \leq 5\mu\text{m}$. Statistically significant flux is not detected in any of these data, including our independent re-analysis of P04’s discovery H - and K -band data. The 3σ detection thresholds are: $F(\lambda_{\text{obs}}=0.44\mu\text{m}) \gtrsim 4.5 \times 10^{-19} \text{ erg s}^{-1} \text{ cm}^{-2}$ per spectral resolution element, $R_{702} \geq 27.0$, $H \geq 25.0$, $K \geq 25.0$, $F(3.6\mu\text{m}) \leq 0.75\mu\text{Jy}$ and $F(4.5\mu\text{m}) \leq 0.75\mu\text{Jy}$, where the photometric limits are calculated in apertures with a diameter 3 \times that of the seeing disk.

Combining these results with those of Bremer et al. (2004)

and Weatherley et al. (2004), we are therefore forced by the data to conclude that there is no statistically sound evidence for the existence of #1916. We also show that inefficient bad-pixel rejection and issues relating to the calculation of the background noise can broadly account for the differences between P04's near-infrared photometry and our own using the same data. The balance of probability is therefore that #1916 was a false detection in P04's analysis. From a broader perspective, the demise of #1916 warns of the hazards of operating close to the detection threshold of deep ground-based near-infrared data.

The need for gravitational magnification to boost the observed flux of faint ($L \lesssim 0.1 L^*$) galaxies at $z \sim 6-8$ and populations of galaxies at still higher redshifts (see §1) is undiminished by our results on #1916. However an important issue is whether it is feasible to find such galaxies using ground-based facilities. We explore this issue using HYPERZ to fit synthetic spectral templates to representative data. Our main conclusions are that deep near-infrared imaging similar to that presented by P04 in combination with a single sensitive optical non-detection from *HST* imaging and moderate depth *Spitzer*/IRAC imaging at 3.6 and $4.5 \mu\text{m}$ can discriminate between low (e.g. $z \sim 2-3$) and high (e.g. $z \gtrsim 7$) redshift solutions with strong statistical significance. In summary, ground-based near-infrared surveys of massive galaxy cluster lenses

with 10-m class telescopes remain a powerful tool for the discovery of intrinsically faint galaxies ($L \lesssim 0.1 L^*$) at $z > 7$ that may be responsible for cosmic re-ionization. Future surveys should combine these data with sensitive space-based optical and mid-infrared observations.

ACKNOWLEDGMENTS

We acknowledge the bold efforts of Roser Pelló and collaborators, and GPS acknowledges cordial discussions with Roser in Lausanne during the summer of 2004. Special thanks go to Jean-Paul Kneib for making the raw near-infrared imaging data available. GPS acknowledges the Caltech Optical Observatories TAC for enthusiastic support, and thanks Richard Ellis and Avishay Gal-Yam for helpful comments on drafts of the manuscript. Thanks also go to Malcolm Bremer, Michael Cooper, Joe Jensen, Dan Stark, Chuck Steidel and Dave Thompson for a variety of discussions and assistance. DJS thanks Dawn Erb, Alice Shapley, Naveen Reddy and Tommaso Treu for assistance with the LRIS data reduction, and acknowledges financial support from NASA's Graduate Student Research Program under NASA grant NAGT-50449. DS and PRME acknowledge support from NASA. We recognize and acknowledge the cultural role and reverence that the summit of Mauna Kea has within the Hawaiian community. We are fortunate to conduct observations from this mountain.

REFERENCES

- Barger A.J., Cowie L.L., Capak P., Alexander D.M., Bauer F.E., Fernandez E., Brandt W.N., Garmire G.P., Hornschemeier A.E., 2003, *AJ*, 126, 632
- Becker R.H., Fan X., White R.L., Strauss M.A., Narayanan V.K., Lupton R.H., Gunn J.E., Annis J., Bahcall N.A., Brinkmann J., et al., 2001, *AJ*, 122, 2850
- Bolzonella M., Miralles J.-M., Pelló R., 2000, *A&A*, 363, 476
- Blain A.W., Chapman S.C., Smail I., Ivison R., 2004, *ApJ*, 611, 725
- Borys C., Chapman S., Donahue M., Fahlman G., Halpern M., Kneib J.-P., Newbury P., Scott D., Smith G.P., 2004, *MNRAS*, 352, 759
- Bouwens R.J., Thompson R.I., Illingworth G.D., Franx M., van Dokkum P.G., Fan X., Dickinson M.E., Eisenstein D.J., Rieke M.J., 2004, *ApJ*, 616, L79
- Bremer M.N., Jensen J.B., Lehnert M.D., Förster-Schreiber N.M., Douglas L., 2004, *ApJ*, 615, L1
- Bruzual A.G., Charlot S., 1993, *ApJ*, 405, 358
- Bunker A.J., Stanway E.R., Ellis R.S., McMahon R.G., 2004, *MNRAS*, 355, 374
- Calzetti D., Armus L., Bolin R.C., Kinney A.L., Koornneef J., Storchi-Bergmann T., 2000, *ApJ*, 553, 682
- Casertano S., de Mello D., Dickinson M., Ferguson H.C., Fruchter A.S., Gonzalez-Lopezlira R.A., Heyer I., Hook R.N., Levay Z., Lucas R.A., et al., 2000, *AJ*, 120, 2747
- Edge A.C., Smith G.P., Sand D.J., Treu T., Ebeling H., Allen S.W., van Dokkum P.G., 2003, *ApJ*, 599, L69
- Egami E., Kneib J.-P., Rieke G.H., Ellis R.S., Richard J., Rigby J., Papovich C., Stark D., Santos M.R., Huang J.-S., et al., 2005, *ApJ*, 618, L5
- Ellis R.S., Santos M.R., Kneib J.-P., Kuijken K., 2001, *ApJ*, 560, L119
- Eyles L., Bunker A., Stanway E., Lacy M., Ellis R.S., Doherty M., 2005, *MNRAS*, submitted, astro-ph/0502385
- Fan X., Narayanan V.K., Strauss M.A., White R.L., Becker R.H., Pentericci L., Rix H.-W., 2002, *AJ*, 123, 1247
- Fan X., Narayanan V.K., Lupton R.H., Strauss M.A., Knapp G.R., Becker R.H., White R.L., Pentericci L., Leggett S.K., Zoltán H., et al., 2001, *AJ*, 122, 2833
- Fazio G.G., Hora J.L., Allen L.E., Ashby M.L.N., Barmby P., Deutsch L.K., Huang J.-S., Kleiner S., Marengo M., Megeath S.T., et al., 2004, *ApJS*, 154, 10
- Franx M., Illingworth G.D., Kelson D.D., van Dokkum P.G., Tran K.-V., 1997, *ApJ*, 486, L75
- Hu E.M., Cowie L.L., McMahon R.G., Capak P., Iwamuro F., Kneib J.-P., Maihara T., Motohara K., 2002, *ApJ*, 568, L75
- Ivison R.J., Smail I., Barger A.J., Kneib J.-P., Blain A.W., Owen F.N., Kerr T.H., Cowie L.L., 2000, *MNRAS*, 315, 209
- Kneib J.-P., Ellis R.S., Santos M.R., Richard J., 2004, *ApJ*, 607, 697
- Kneib J.-P., van der Werf P.P., Kraiberg Knudsen K., Smail I., Blain A.W., Frayer D., Barnard V., Ivison R., 2004, *MNRAS*, 349, 1211
- Kogut A., Spergel D.N., Barnes C., Bennett C.L., Halpern M., Hinshaw G., Jarosik N., Limon M., Meyer S.S., Page L., Tucker G.S., Wollack E., Wright E.L., 2003, *ApJS*, 148, 161
- Labbé I., Franx M., Rudnick G., Förster Schreiber N.M., Rix H.-W., Moorwood A., van Dokkum P.G., van der Werf P., Röttgering H., van Starkenburg L., et al., 2003, *AJ*, 125, 1107
- Lehnert M.D., Förster Schreiber N.M., Bremer M.E., 2004, *ApJ*, submitted, astro-ph/0412432
- Madau P., 1995, *ApJ*, 441, 18
- Mellier Y., Fort B., Soucail G., Mathez G., Cailloux M., 1991, *ApJ*, 380, 334
- Oke J.B., 1990, *AJ*, 99, 1621
- Oke J.B., Cohen J.G., Carr M., Cromer J., Dingizian A., Harris F.H., 1995, *PASP*, 107, 375
- Pelló R., Schaerer D., Richard J., le Borgne J.-F., Kneib J.-P., 2004, *A&A*, 416, L35
- Richard J., Schaerer D., Pelló R., le Borgne J.-F., Kneib J.-P., 2003, *A&A*, 412, 57
- Sand D.J., Treu T., Ellis R.S., 2002, *ApJ*, 574, L129
- Sand D.J., Treu T., Smith G.P., Ellis R.S., 2004, *ApJ*, 604, 88
- Sand D.J., Treu T., Ellis R.S., Smith G.P., 2005, *ApJ*, accepted
- Santos M.R., Ellis R.S., Kneib J.-P., Richard J., Kuijken K., 2004, *ApJ*, 606, 683
- Schlegel D.J., Finkbeiner D.P., Davis M., 1998, *ApJ*, 500, 525
- Sharon K., Ofek E.O., Smith G.P., Broadhurst T., Maoz D., Kochanek C., Oguri M., Suto Y., Inada N., Falco E.E., 2005, *ApJL*, 629, 73
- Smail I., Ivison R.J., Blain A.W., Kneib J.-P., 2002, *MNRAS*, 331, 495
- Smail I., Smith G.P., Ivison R.J., 2005, *ApJ*, in press, astro-ph/0506176
- Smith G.P., Kneib J.-P., Ebeling H., Czoske O., Smail I., 2001, *ApJ*, 552, 493
- Smith G.P., Smail I., Kneib J.-P., Davis C.J., Takamiya M., Ebeling H., Czoske O., 2002, *MNRAS*, 333, L16
- Smith G.P., Kneib J.-P., Smail I., Mazzotta P., Ebeling H., Czoske O., 2005, *MNRAS*, 359, 417
- Steidel C.C., Giavalisco M., Pettini M., Dickinson M.E., Adelberger K.L., 1996, *ApJ*, 462, L17
- Stern D., Eisenhardt P., Spinrad H., Dawson S., van Breugel W., Dey A., de Vries W., Stanford S.A., 2000, *Nature*, 408, 560
- Weatherley S.J., Warren S.J., Babbedge T.S.R., 2004, *A&A*, 428, L29
- Yan H., Windhorst R., 2004, *ApJ*, 600, L1